Clim Dyn (2011) 36:2201–2218
DOI 10.1007/s00382-010-0795-1

An Antarctic view of Beryllium-10 and solar activity for the past millennium

Gilles Delaygue · Edouard Bard

Received: 24 October 2009 / Accepted: 10 March 2010 / Published online: 1 April 2010
© Springer-Verlag 2010

Abstract Beryllium-10 in ice provides a valuable proxy of solar activity. However, complex production pathways, atmospheric transport, and deposition processes impede its quantitative interpretation. Here, we examine the influence of deposition processes on two Be-10 ice core records from Central Antarctica (South Pole and Dome Fuji stations), covering the last millennium. We try to quantify how Be-10 variations in ice relate to variations in Be-10 production, and the bias associated to this relationship. An independent bias estimation is provided by comparing atmospheric radiocarbon variations reconstructed from tree rings and deduced from Be-10 variations. Both techniques suggest an uncertainty of the order of 10% in Be-10 production. This uncertainty estimate does not account for the geographical origin of Be-10, which remains a major issue. Because both Be-10 records are so similar, we propose to average them as a means to decrease the unshared (non solar) variability. This average record provides a new reconstruction of solar modulation parameter Φ and total solar irradiance over the last ~1,300 years. The lowest solar activity is found during the so-called Spörer Minimum (around AD 1450). The highest activities are found during the 8th century and over the last decades: as shown in previous studies, our results suggest that the recent solar activity is not exceptionally high for the last millennium.

Keywords Beryllium-10 · Solar activity · Ice cores · Antarctica · Paleoclimate

1 Introduction

The response of global surface temperature to climatic forcings, the so-called climatic sensitivity, is a key parameter for climate projections over the next century. Estimating this sensitivity requires to reconstruct temperature variations and climatic forcings from the past. Typically, the large climatic variation of the last glacial-interglacial transition has been used (e.g., Joussaume and Taylor 1995), but the definition of the associated forcings is not straightforward (e.g., Hansen et al. 2008). The last millennium, with better constrained forcings, has also been used for such estimate, but the small amplitude of the temperature change requires that the concomitant forcing is known with high accuracy. In addition, simulations of the climatic changes associated with this period have shown that regional differences have to be accounted for when estimating the global temperature change (e.g., Shindell et al. 2003). Climate simulations are thus essential complements to measurements for estimating past global temperature change.

For the past millennium, variations of the total solar irradiance (TSI) have been recognized as a primary climatic forcing. Volcanic eruptions have had a strong climatic impact but limited in time. These TSI variations are

Electronic supplementary material The online version of this article (doi:10.1007/s00382-010-0795-1) contains supplementary material, which is available to authorized users.

G. Delaygue · E. Bard
Université Aix-Marseille III/CNRS/IRD/Collège de France, CEREGE, Europôle de l'Arbois BP80, 13545 Aix-en-Provence Cedex4, France

Present Address:
G. Delaygue (✉)
Université Joseph Fourier-Grenoble I/CNRS, LGGE, 54 rue Molière, 38402 Saint-Martin-d'Hères Cedex, France
e-mail: delaygue@lgge.obs.ujf-grenoble.fr

reconstructed from proxies of solar activity, mainly sunspot number and cosmogenic isotope (^{14}C, ^{10}Be) concentration. Each proxy has advantages and drawbacks. Sunspot number depends on the so-called 'closed' solar magnetic flux which is directly linked to TSI (e.g., Wang et al. 2000). Yet, the sunspot number record is limited to the past 400 years, and sunspot number is not simply related to solar activity: (i) minima of the 11-year cycle do not show significant centennial trend, contrary to other indices like the Aa index, one of the best indices of recent solar magnetic activity (e.g., Lockwood and Stamper 1999), and (ii) during Grand Minima, i.e., periods of persistent solar quiescence like the Maunder Minimum, hardly any sunspots were observed during decades whereas other indices suggest that a solar activity modulation persisted (e.g., Beer et al. 1998). On the other hand, cosmogenic isotope records, mainly ^{14}C and ^{10}Be, cover several millennia and show continuous variations, especially during solar minima. In particular, the IntCal04 reconstruction of atmospheric carbon-14 content, based on tree rings, extends over several millennia with a 5-year time resolution (Reimer et al. 2004). These cosmogenic isotope records suggest that a solar activity modulation persisted during the Maunder Minimum (e.g., Stuiver and Braziunas 1993; Beer et al. 1998; Berggren et al. 2009). Yet, the cosmogenic isotope production depends on the interplanetary magnetic field and thus on the so-called 'open' solar magnetic flux, as for aurorae and *Aa* index: this dependence makes these proxies less directly linked to TSI than the sunspot number. However, Fröhlich (2009) claims that the three observed TSI minima do show a significant trend, which is only found in the 'open' magnetic flux. This suggests that part of the long-term (centennial) trend in TSI may be recorded by cosmogenic isotopes.

Using carbon-14 as a proxy of solar activity has two drawbacks. First the global carbon cycle damps and delays atmospheric ^{14}C variations compared to the corresponding production variations, and this must be corrected for by using a carbon cycle model. Especially, the very strong 11-year solar cycle is hardly measured in records of atmospheric ^{14}C because it is so much damped (e.g., Stuiver and Braziunas 1993). We show in Sect. 4 how much uncertainty remains on this correction of the carbon cycle effects. Secondly, anthropogenic activities have considerably modified the atmospheric content of ^{14}C over the last century through emissions of ^{14}C-free CO_2 and production of ^{14}C by nuclear explosions. This complicates the estimation of natural ^{14}C production over this period and its comparison with satellite TSI measurements (e.g., Solanki et al. 2005).

Beryllium-10 does not present these drawbacks of carbon-14 because it is deposited to the surface very quickly (within a year after its production) and has not been noticeably altered by anthropogenic activities. A technical limitation of its use is that it is measured in snow and ice with a typical time resolution of several decades, which smoothes out the very strong 11-year solar cycle. The large quantity of ice required for ^{10}Be measurements has so far limited the possibility of documenting the 11-year solar cycles over several centuries to high accumulation sites (Beer et al. 1990; Berggren et al. 2009). The application of higher energy mass spectrometer to ice samples from coring sites with intermediate/low accumulation rate should help produce long ^{10}Be records at sub-decadal resolution.

Besides this technical limitation, the main source of uncertainty for interpreting ^{10}Be concentration in terms of solar activity is its atmospheric transport and deposition. Both processes influence the ratio between wet and dry deposition modes, and thus the extent to which the ^{10}Be deposition flux represents solar activity. In this regard, the central Antarctic Plateau combines two advantages: (i) ^{10}Be deposition is very sensitive to solar activity and much less so to geomagnetism, (ii) and ^{10}Be deposition is arguably more stable than anywhere else (see discussion in Bard et al. 1997). We discuss both points in Sect. 3. Raisbeck et al. (1990) have produced a ^{10}Be record from the South Pole station covering the last millennium. More recently, Horiuchi et al. (2008) have published a new record from the Dome Fuji station, on the Antarctic Plateau, covering approximately the same period. Both records have been shown to compare quite well with ^{14}C variations (Bard et al. 1997; Horiuchi et al. 2008), which suggests that they are good proxies of solar activity. Usoskin et al. (2009) have estimated the coherence of both records, as well as their coherence with a reconstruction of ^{14}C production. They found high levels of coherence at periods longer than about 80–100 years, but irregular levels of coherence at shorter periods. The latter feature is either due to dating error and/or to 'unforced' variability specific to each record (i.e., variability not related to solar activity, but due to changes in deposition mode and/or snow accumulation). We discuss the respective chronology of each record in Sect. 2, and the deposition mode of ^{10}Be in Sect. 3, with the aim to estimate the uncertainty in the reconstructed solar variability due to chronological errors and accumulation change. As a means to remove part of the 'unforced' variability, the two ^{10}Be normalized records are averaged ('stacked'), as described in Sect. 2. We then compare in Sect. 4 the individual ^{10}Be records and the ^{10}Be stack with ^{14}C variations in order to independently estimate the uncertainty in using ^{10}Be as a solar proxy. Eventually, in Sect. 5 we propose a reconstruction of solar variability based on the ^{10}Be stack.

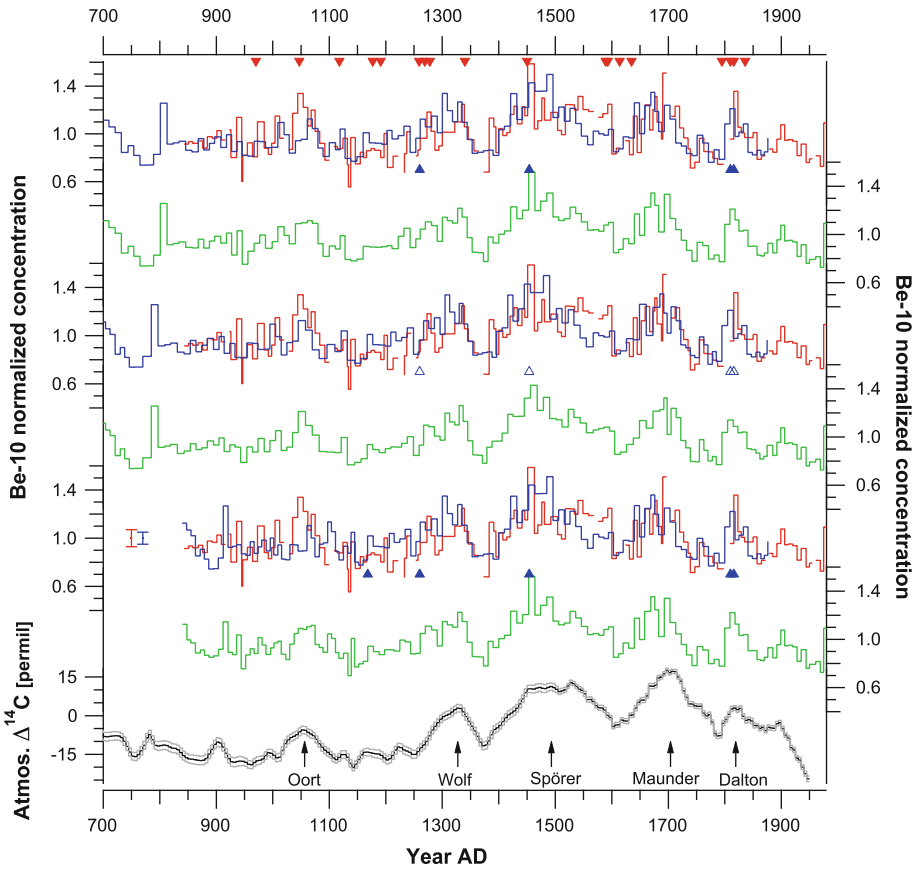

Fig. 1 Beryllium-10 concentration records and stacks, plotted with three different timescales, compared to atmospheric ^{14}C variations. The South Pole ^{10}Be concentration record is plotted in red, the Dome Fuji concentration record in blue, their stack in green, the IntCal04 ^{14}C atmospheric content reconstruction for the northern hemisphere in black (Reimer et al. 2004; with the $\pm 1\sigma$ precision as *grey curves*). The chronology of the South Pole record is the one published by Bard et al. (1997), based on volcanic eruptions (*red triangles*). The chronologies of the Dome Fuji record and of the stack are based on volcanic eruptions (*blue triangles*). *Top*: the chronology is based on 5 eruptions (initial dating of Horiuchi et al. 2008, note that the fifth eruption at year 360 BC is out of the plot); *Middle*: it is adjusted by correlation with ^{14}C production (published timescale of Horiuchi et al. 2008); *Bottom*: it is based on three additional eruptions proposed by Motizuki et al. The analytical 2σ precision on the ^{10}Be measurements is represented by the vertical bars. *Arrows* underline minima of solar activity, also attested by other solar proxies

2 Materials and methods

2.1 Beryllium-10 records from South Pole and Dome Fuji

The South Pole record (Raisbeck et al. 1990; Fig. 1) has been acquired on the 127 m long PS1 ice core drilled in 1984 at the South Pole station (elevation 2,835 m, annual mean temperature −49°C). It consists in 144 measurements of ^{10}Be concentration on 80 cm long samples (~1 kg), with a typical analytical precision of 7%. Along the core, several tens of centimeters of ice were not used for measurements, for a total of 12 m of ice (less than 10%). Hence, the ^{10}Be record does not exactly represent the whole period covered by the ice core, which approximately spans year 840 AD to year 1980 AD (Anno Domini i.e., of this era). The record has a near decadal resolution (average of 8 years) corresponding to a mean accumulation rate of about 7 cm water equivalent per year. The identification of 20 eruptions has allowed Delmas et al. (1992) to date the ice with a precision ranging between 2 and 10 years, depending on the age. The chronology for PS1 has been slightly modified (Bard et al. 1997), based on the age revision of six of these eruptions (R. Delmas, personal communication). This revision amounts to less than 10 years.

The Dome Fuji record (Horiuchi et al. 2007; Horiuchi et al. 2008; Fig. 1) has been acquired on the 122 m long DF2001 ice core drilled in 2001 at the central Antarctica Dome Fuji station (77°19′S–39°42′E, elevation 3,810 m, 10 m depth temperature of −58°C). It consists in 121 measurements of ^{10}Be concentration made continuously about every 50 cm long samples (~200 g), with an analytical precision better than 5%. The record approximately covers the period of years 695–1875 AD, with a decadal resolution (average of 10 years) corresponding to an average accumulation of about 2.5–3 cm water equivalent

per year. An initial dating of the ice based on the identification of eruptions was proposed by Horiuchi et al. (2007), with a precision of about 10 years. Since no eruption was identified over the period ranging from 346 BC (Before Christ) to 1260 AD (open blue triangles on Fig. 1), the chronology of the ice is loose over this long period of more than 1,500 years. Because the ^{10}Be variations so closely follow ^{14}C variations, Horiuchi et al. (2008) have slightly adjusted this initial chronology by correlating the ^{10}Be record with a ^{14}C production reconstruction. This adjustment amounts to a few years after 1260 AD, and up to 50 years before. Since our aim is to test the validity of the ^{10}Be record as a proxy of the ^{14}C production, a chronology partly based on this production should not be used, although the adjustment is very small. For this reason, we have tried to include additional age markers in order to refine the loosely dated period before year 1260 AD. Motizuki et al. (submitted manuscript available at http://arxiv.org/abs/0902.3446, version 1) have identified 3 additional eruptions in this DF2001 core, at depths 85.61, 70.29 and 42.48 m, corresponding, respectively, to years 180, 639 and 1168 AD. These additional tie points considerably affect the depth-age relationship with a slope (apparent accumulation rate) over the period of years 639–1168 AD which is 40% higher than before and after. This increase is consistent with thicker snow layers (potentially annual layers) observed over this period by Narita et al. (2003) in a companion core (but see discussion in the next section). We have used the last two dates (years 639 and 1168 AD) to propose a third chronology of the Dome Fuji ^{10}Be record before year 1260 AD.

Figure 1 shows the ^{10}Be concentration records of South Pole and Dome Fuji, normalized to their own average over their common period, plotted with independent chronologies. The Dome Fuji record is presented with the three different chronologies discussed above. The correspondence of these relative variations appears to be quite good, both in time and amplitude, when considering both the number of processes determining these concentrations as well as the accumulation contrast between both sites (in a ratio of $\sim$2.6). To quantify the correlation between the two ^{10}Be records, we have resampled them with a 10-year timestep in order to calculate their correlation. The linear correlation coefficient r between the Dome Fuji record and the South Pole record is 0.67 using the Dome Fuji initial chronology, $r = 0.69$ using the ^{14}C adjusted chronology, and $r = 0.60$ with the two additional eruptions (in these three cases $n = 104, p < 0.001$). The correspondence of the ^{10}Be variations in each record is also good at the century timescale with the variations of atmospheric ^{14}C (bottom of Fig. 1). This strengthens the hypothesis that the recorded variations are mainly due to a common origin: the production of ^{10}Be in the atmosphere (Raisbeck et al. 1990).

2.2 Difference between ^{10}Be records and possible causes

2.2.1 *Difference due to the chronologies*

Still, some differences are obvious between the South Pole and the Dome Fuji ^{10}Be concentration records, which may be partly due to dating bias. The chronology of the South Pole core is based on 20 eruptions (red triangles on Fig. 1), but only 4 of these eruptions are used for the initial chronology of the Dome Fuji core (blue triangles on Fig. 1), plus a much older one at year 346 BC. The two eruptions added from Motizuki et al. (blue triangles at years 639 and 1168 AD) make the bottom of the record younger by several centuries (third plot of Fig. 1). From the visual inspection of Fig. 1, and as confirmed by correlation (see above), it is clear that both chronologies of Horiuchi et al. (2008) (i.e., with and without ^{14}C adjustment) give the best correspondence with both the South Pole ^{10}Be and the atmospheric ^{14}C records. Especially, the correspondence during the solar Oort Minima is greatly improved by using the ^{14}C adjusted chronology. On the contrary, using the additional two eruptions of Motizuki et al. slightly degrades the correspondence between the bottom parts of the records, although the ^{10}Be variations are small in these parts: (i) the relative maxima of the Dome Fuji record around the Oort Minimum are not in line with the relative maxima of the South Pole ^{10}Be and the ^{14}C records; and (ii) the bottom part of the Dome Fuji record is out of phase with the ^{14}C record before *ca.* year 1000 AD. Hence, the chronology proposed by Motizuki et al. does not seem to be supported by the ^{10}Be record. In fact, in a companion core, Narita et al. (2003) found a more limited increase of snow accumulation (by 15% instead of 40%) over a period roughly spanning years 700–1100 AD. This argument, as well as the poorer correlation between both ^{10}Be records using the third chronology for the Dome Fuji record, suggest that the identification of volcanic eruptions by Motizuki et al. may not be correct.

2.2.2 *Difference due to unforced variability*

Figure 1 also shows that 'wiggle-matching' the South Pole and Dome Fuji ^{10}Be records, to correct chronological difference, cannot improve their correlation for some periods, especially for the 15th and 16th centuries during which the ^{10}Be relative levels are different. Hence, some unforced variability (i.e., not solar) at the multidecadal scale also contributes to these differences, probably related to deposition processes (variations in snow accumulation and/or change in the mode of ^{10}Be deposition). Bursts of solar rays would produce spikes in the ^{10}Be flux at the annual scale (Usoskin et al. 2006a; Webber et al. 2007), but this

would equally affect ^{10}Be records at South Pole and Dome Fuji, thus increasing their correlation. Hence, local processes probably explain most of the disagreement observed between both ^{10}Be records. As discussed below, it is very difficult to correct for these processes: this is why we propose to average both records in order to smooth out part of this unforced variability.

2.3 A stack of the Beryllium-10 records

The 'stack' is calculated as the average of the relative variations in ^{10}Be concentration (Fig. 1). The relative variations were simply calculated by dividing each concentration value by the long term average of the individual records over the period of years 843–1876 AD. We did not normalize the ^{10}Be records with respect to standard deviation, because (i) these relative variations should represent relative variations of ^{10}Be production (cf Sect. 3), and (ii) both ^{10}Be records are expected to be equally sensitive to solar activity due to the high latitudes of the drilling sites. The standard deviations of the records are actually very close: 0.16 and 0.19 for the Dome Fuji and South Pole ^{10}Be concentration, respectively.

For averaging, we account for the period of time covered by each sample. These periods are different between the two cores because of different ice sample length (50 vs. 80 cm) and some gaps (<10 cm) in South Pole ice sampling. We use the time intervals of the Dome Fuji record and average the ^{10}Be values which overlap each interval (proportionally to the overlap). The last $\sim$100 years of the stack is only made of the South Pole record, and with the first two chronologies adopted for the Dome Fuji core (Fig. 1), the first $\sim$150 years of the stack is only made of the Dome Fuji record.

The good correspondence between the South Pole and Dome Fuji ^{10}Be records may be specific to the East Antarctic plateau. Hence we have to show that they are indeed reliable solar proxies i.e., that a quantitative relationship does exist between ^{10}Be concentration in ice cores from this region and solar variability. These questions are far from being solved, and in the following sections we address them in two ways: firstly by evaluating the relationship between ^{10}Be flux and concentration in snow (Sect. 3), secondly by comparing ^{10}Be variations with variations in atmospheric radiocarbon, which is another cosmogenic isotope related to solar activity (Sect. 4).

3 Beryllium-10 concentration as a quantitative proxy of solar activity

As discussed by Bard et al. (1997, 2007), several factors make the East Antarctic Plateau a favorable area to record variations of solar activity: a high geomagnetic latitude, a limited climatic variability at several timescales, and a dominant deposition mode by aerosols. The high latitude location maximizes the sensitivity of ^{10}Be concentration to solar activity relative to that to geomagnetism. Over the last millennium the geomagnetic South pole has wandered by about 20° around the geographic South pole, but both stations have remained at a high geomagnetic latitude (McCracken 2004). The limited climatic impact is supported by the modelling work of Field and Schmidt (2009), who have found a lower impact of unforced, weather-related changes on ^{10}Be concentration on the East Antarctic Plateau compared to Central Greenland. We review here available data of ^{10}Be concentration and of snow accumulation in order to estimate the purely climatic (non solar) variability of ^{10}Be records in the former region.

3.1 Relationship between ^{10}Be concentration and snow accumulation

The atmospheric residence time of ^{10}Be, of the order of 1 year (e.g., Raisbeck et al. 1981), is short compared to the decadal/centennial variations we are interested in. Hence we thus assume that variations in ^{10}Be atmospheric concentrations are proportional to variations in ^{10}Be production. Since beryllium is attached to aerosols, the ^{10}Be flux to the surface is in the form of aerosols, which are largely dominated by sulfate on the Antarctic Plateau (e.g., Shaw 1988). These aerosols are either deposited directly to the surface (dry deposition) or scavenged by precipitation (wet deposition).

The dry flux of ^{10}Be (Fd, e.g., in atoms/m^2/s) is due to the deposition of sulfate particles (with a speed Kd, e.g., in m/s) from an atmospheric reservoir (with a concentration Ca in atoms/m^3) (see, e.g., Legrand 1987). In the hypothetical case of purely dry deposition, the ^{10}Be concentration in snow (Cs, e.g., in atoms/kg of water) is determined by the dilution of the dry flux by the snow accumulation (b in kg of water/m^2/s):

$$\mathrm{Cs} = \mathrm{Fd}/\mathrm{b} = \mathrm{Kd} \times \mathrm{Ca}/\mathrm{b}. \quad (1)$$

On the other hand, in the hypothetical case of purely wet deposition, ^{10}Be concentration in snow (Cs) is determined by its atmospheric concentration (Ca), the precipitation rate, and a scavenging efficiency (kw, dimensionless). Since sublimation does not appreciably modify the net accumulation on the Antarctic Plateau (e.g., Kameda et al. 1997), the precipitation and accumulation rates are similar, and the ^{10}Be flux by wet deposition (Fw) reads:

$$\mathrm{Fw} = \mathrm{kw} \times \mathrm{Ca} \times \mathrm{b}, \quad (2)$$

and the ^{10}Be snow concentration:

$$Cs = Fw/b = kw \times Ca. \quad (3)$$

In reality, both dry and wet deposition modes contribute to the total ^{10}Be flux:

$$F = Fd + Fw = Kd \times Ca + kw \times Ca \times b. \quad (4)$$

Hence the ^{10}Be concentration in snow (Cs) is proportional to the ^{10}Be concentration in air (Ca) only if the other parameters are constant:

$$Cs = F/b = Kd \times Ca/b + kw \times Ca = (Kd/b + kw) \times Ca. \quad (5)$$

Equations 1–5 apply to sulfate as well. Observations have shown, for a variety of Antarctic and Greenland sites, that time averaged ^{10}Be and sulfate fluxes in the firn are to a first order proportional to the snow accumulation, as expected from Eq. 4 (e.g., Raisbeck and Yiou 1985; Delmas 1992; Legrand 1995). Figure 2 shows such empirical relationships for different Antarctic sites. Most of the sites used for ^{10}Be have very low accumulation, and the strongest correlation is found between ^{10}Be concentration and the inverse of the accumulation, as expected from Eq. 5 ($r^2 = 0.92$ compared to $r^2 = 0.85$ for the correlation between ^{10}Be flux and accumulation, $n = 18$). In this data compilation, snow accumulation and ^{10}Be concentration were averaged over the same time period. When possible, for each site, different time periods have been used to increase the number of data. For sulfate, several sites have higher accumulation, and the strongest correlation is found between sulfate flux and accumulation ($r^2 = 0.97$, $n = 13$). Besides, a very strong correlation does exist between sulfate and ^{10}Be concentrations (Delmas 1992), even for the limited Antarctic dataset ($r^2 = 0.9$, $n = 4$, not shown). The correlation is even stronger when adding Greenland data ($r^2 = 0.98$, $n = 6$, not shown, see Delmas 1992). These linear correlations suggest that:

(i) the dry flux Fd (intercept in Eq. 4 or slope in Eq. 5) is rather homogeneous over Antarctica (and maybe over the polar regions) for both ^{10}Be and sulfate;

(ii) the dry fluxes are 65 ± 5 ^{10}Be atoms/m^2/s (slope of the linear regression in Eq. 5) and 2 ± 0.3 kg/km^2/year of sulfate (intercept of the linear regression in Eq. 4);

(iii) both ^{10}Be and sulfate give slightly different estimates of the dry flux proportion: this proportion is systematically 10–20% lower for the sulfate flux than for the ^{10}Be flux. Due to the paucity of data, it is difficult to discuss whether this difference is significant or not. Delmas (1992) noticed that the linear regression of ^{10}Be against sulfate concentrations yields an intercept different from zero, which may suggest some decoupling between ^{10}Be and sulfate fluxes. However, this feature does not hold for Antarctic data, so that more data are required to discuss this hypothesis.

(iv) The dry deposition of sulfate predominates (>66%) at sites where the total flux of sulfate is less than ~3 kg/km^2/year. For ^{10}Be, the dry deposition predominates at sites where the total flux is less than ~100 atoms/m^2/s. This is generally the case for area with low accumulation (<10 cm water equivalent/year), typical of the Antarctic Plateau.

(v) Accounting for the uncertainties in the slope and intercept of the linear regressions, the dry flux is estimated to represent 52 ± 8% of the sulfate flux

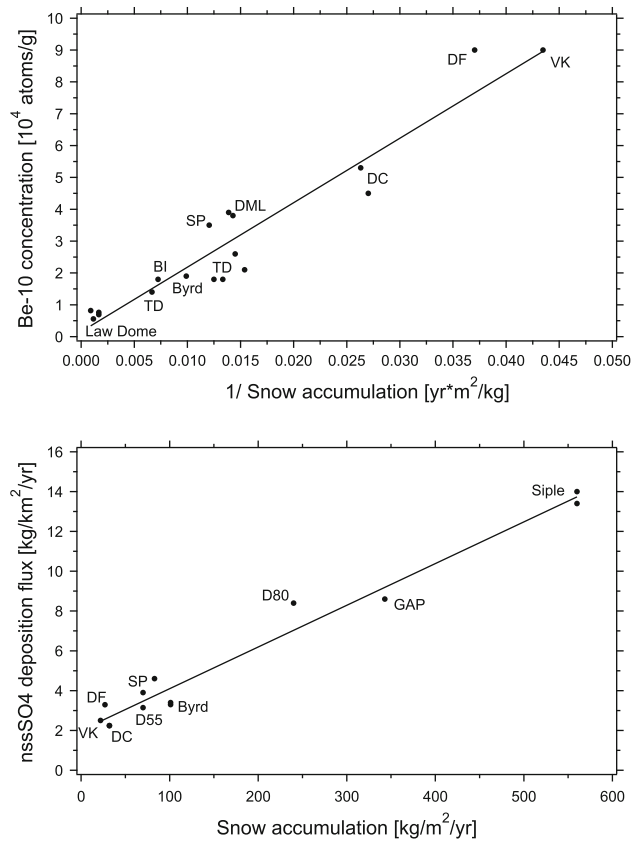

Fig. 2 Relationship between snow accumulation and ^{10}Be concentration or sulfate flux for several sites in Antarctica. Multiple points for a same site correspond to different time periods or different surface samples. *Top*: Beryllium-10 concentration versus the inverse of accumulation. The linear regression gives a correlation coefficient $r^2 = 0.92$ ($n = 18$, $p < 0.0001$). Data from Delmas (1992) augmented by data from Huke et al. (2002) for Dronning Maud Land (DML) and Berkner Island (BI); Beer et al. (1987) for Byrd; Smith et al. (2000) and Pedro et al. (2006) for Law Dome; Steig et al. (1995) for Taylor Dome (TD). *Bottom*: Non-sea-salt sulfate flux versus accumulation. The linear regression gives a correlation coefficient $r^2 = 0.97$ ($n = 13$, $p < 0.005$). Data from Legrand (1995) augmented by data from Kirchner and Delmas (1988) for South Pole (SP; last millennium average with a long term accumulation of 70 mmWeq./year) and from Iizuka et al. (2004) for Dome Fuji (DF). *VK* Vostok, *DC* Dome Concordia

and 71 ± 6% of the ^{10}Be flux at South Pole, and 61 ± 9% of the sulfate flux and 84 ± 6% of the ^{10}Be flux at Dome Fuji.

General circulation models equipped with ^{10}Be or aerosols could also give valuable estimates of the proportions of dry versus wet deposition mode. However, the extreme conditions of the Antarctic Plateau, in terms of climatic conditions as well as transport of aerosols, are not well captured by models. For instance, Field et al. (2006) found that the modelled flux of ^{10}Be to Antarctica is largely dominated by the dry mode (their Fig. 1), except on the Plateau where both modes are of equal importance; this result is in contradiction with the data analysis above. Also, their modelled concentration of ^{10}Be at South Pole is two to three times the observed one. Heikkilä et al. (2009) simulated a flux of ^{10}Be at South Pole about 10 times smaller than the observed one (7 vs. ~80 atoms/m^2/s given by Raisbeck and Yiou 1985). Whereas simulations of ^{10}Be concentration in polar snow are very useful for sensitivity tests, realistic values in Antarctica seem still out of grasp.

3.2 Can we correct ^{10}Be concentration for accumulation change?

If the above interpretation of sulfate and ^{10}Be data in terms of deposition modes is correct, then dry deposition would be dominant in the total flux of ^{10}Be to the Antarctic Plateau, with wet deposition contributing to 20–30%. Hence, ^{10}Be concentration in snow is a quantitative proxy of ^{10}Be atmospheric production only if all other parameters (Kd, kw, b in Eq. 5) have been constant or can be reconstructed.

Discussion of Kd and kw variability is clearly beyond the scope of this study. Measurements of aerosol concentrations simultaneously in free air and in snow have shown that their relationship strongly varies with seasons, being mostly controlled by the temperature inversion regime (e.g., Shaw 1988; Bergin et al. 1998). Also, the dry deposition flux of aerosols may be controlled by wind 'filtering' through the surface snow ('wind pumping', e.g., Harder et al. 2000). Hence, several mechanisms may influence Kd and kw, and their variability at the decadal/centennial scales is difficult to address. The fact that the very good correlations shown in Fig. 2 are obtained with data from different periods of time only suggests that Kd and kw may have been approximately constant. Here we actually assume that Kd and kw have been constant in the past at the decadal and centennial timescales.

On the other hand, changes in accumulation (b) did affect ^{10}Be concentration (in proportion of the dry flux, cf Eq. 5), and it should be possible to correct ^{10}Be concentration for these changes. However, this correction is not possible in our case for three reasons:

(i) snow accumulation record is not available at the decadal/centennial timescale for either of the South Pole or Dome Fuji ice cores;

(ii) comparison of snow accumulation records from nearby cores in Antarctica has shown poor similarity at the decadal/centennial scales (e.g., Jouzel et al. (1983) and van der Veen et al. (1999) for South Pole; Kameda et al. (2008) for Dome Fuji; Ekaykin et al. (2004) for Vostok), which is probably related to the existence of snow dunes affecting accumulation at the 10–100 m scale;

(iii) water isotopes represent a poor proxy of accumulation at these decadal/centennial timescales, as shown by Jouzel et al. (1983) at South Pole, and Ekaykin et al. (2002) and Ekaykin et al. (2004) at Vostok. Horiuchi et al. (2008) have used this proxy to reconstruct an accumulation record for the Dome Fuji ice core, based on the spatial relationship between water isotopes and accumulation observed along a traverse of East Dronning Maud Land by Satow et al. (1999). However, there is no indication that such spatial relationship also holds for the past. In fact, Figs. 3 and 5 of Horiuchi et al. (2008) show ^{10}Be concentration and flux (i.e., corrected for accumulation), and it is not obvious that ^{10}Be flux is better correlated with ^{14}C production than ^{10}Be concentration is.

3.3 Maximum bias due to accumulation change

If a precise correction of accumulation changes is not possible, it is still possible to estimate the magnitude of this correction, that is, the extent to which accumulation changes have modified ^{10}Be concentration. Few records of accumulation exist at the decadal/centennial time resolution covering the last millennium, because reconstructing accumulation is such a difficult task (requiring both to identify time markers and to measure snow density). We are aware of only two of such accumulation records at the South Pole station, based on visual and chemical detection of annual layers, as detailed by Mosley-Thompson et al. (1999). A trend common to both records at the centennial scale can be observed, corresponding to a slow decrease of accumulation (by 20–25%) with a minimum during the 16th to 17th centuries, followed by a more rapid increase of the same amplitude. Such minimum is consistent with cooler conditions over Antarctica estimated from water isotopes during a period referred to as the 'Neoglacial' or the 'Antarctic Little Ice Age' by some authors (e.g., Masson et al. 2000). Assuming that this trend also exists in the PS1 core in which ^{10}Be has been measured, this

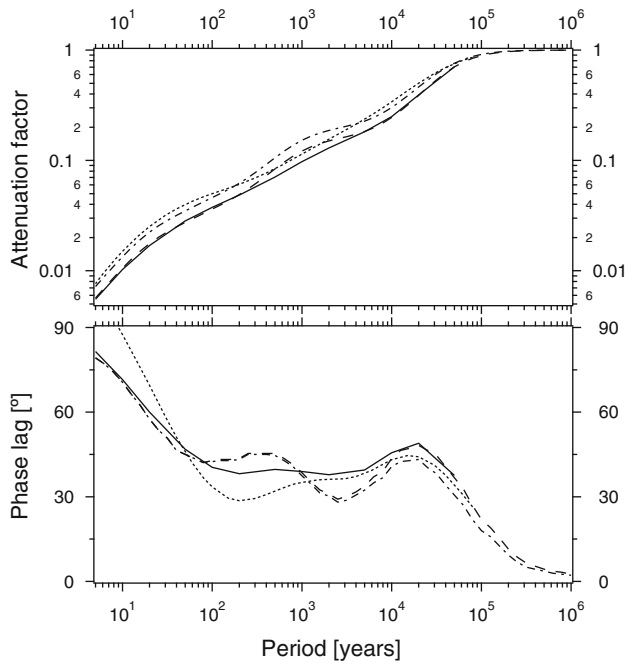

Fig. 3 Simulated attenuation factor (*top*) and phase lag (*bottom*) of atmospheric ^{14}C concentration for sinusoidal variations in ^{14}C production, as a function of the period of these variations, for different carbon models (see characteristics in Table 1). The phase lag is calculated as the time lag divided by the period and multiplied by 360°. *Plain line*: Bern 2D climate model. *Dotted line*: 12 box model. *Dotted-dashed line*: 7 box model. *Dashed line*: 4 box model based on the 7 box model without the sediment boxes

accumulation decrease (20% lower than average) would have increased ^{10}Be concentration by about 15% (assuming that dry flux contributes to ~70% of the total ^{10}Be flux, cf Eq. 5), independently of ^{10}Be production. Hence, solar activity reconstructed from ^{10}Be concentration may be too low by 15% during the 16th and 17th centuries, a period which includes the Maunder Minimum. Conversely, accumulation was probably 5–10% higher than average during the last three centuries, as well as during the 11th and 12th centuries. Solar activity reconstructed from ^{10}Be concentration may thus be too high by 4–7% during this period, which includes two solar high levels during the 18th and 20th centuries.

For the Dome Fuji station, we are only aware of the accumulation reconstruction by Narita et al. (2003) based on the visual identification of layers in a 125 m long ice core. A decreasing trend of accumulation over the last millennium similar to the one described above at South Pole is observed, but with an amplitude of ~60%. In fact, as detailed by Narita et al. the observed layers are probably not annual ones in the top ~30 m of the core, due to the formation of depth hoar in the firn. If their assumption of annual layers below ~30 m is valid, it would imply an accumulation rate about 20–40% higher than average during the 11th to 13th centuries, which would decrease ^{10}Be concentration by 15–30% (i.e., 84% of 20–40%). This decrease may help explain that variations in ^{10}Be concentration in the Dome Fuji core are smaller during this period than in the South Pole core (Fig. 1), especially the peak associated with the Oort Minima which is 15–20% lower. However, Narita et al. have also estimated accumulation variations based on volcanic stratigraphy at a much lower time resolution: an accumulation rate ~15% higher is found during approximately the 9th to 13th century period (so called 'Medieval Period'). This accumulation estimate is averaged over a much longer period than the estimate based on layer thickness, and both estimates cannot be compared directly. However, we note that: (i) identification of annual layers is always problematic at such low accumulation rate, thus the estimate based on volcanic stratigraphy is expected to be much more reliable, and (ii) the accumulation rate based on layer thickness is still 30–40% higher than the one based on volcanic stratigraphy when averaged over the same 9th to 13th century period. This suggests that the layers observed by Narita et al. are not annual ones. Hence, it seems that a more reliable figure for a possible bias in ^{10}Be production is an underestimate by only ~13% (i.e., 84% of the 15% based on volcanic stratigraphy) during the Medieval Period. This figure is again consistent with the difference with the South Pole ^{10}Be concentration for this period.

Hence, it is probable that climatic trends in snow accumulation did occur at the centennial timescale, and have biased in a systematic way the reconstruction of ^{10}Be production, but this bias is probably limited to 10–15%. Moreover, even if accumulation reconstructions were to exist in both ice cores, it is not obvious that a correction of ^{10}Be concentration based on Equation 5 would be more precise because (i) the accumulation reconstruction itself may not be reliable, and (ii) accumulation changes have to be weighted by the contribution of dry deposition which is not well known. Considering our limited level of knowledge and the lack of precise accumulation data, averaging the two ^{10}Be concentration records is probably the most efficient way to remove part of this probable bias, keeping in mind that it is limited to 10–15%. We will see in the following that a much stronger uncertainty arises from the geographical origin of ^{10}Be.

A completely independent way to estimate the bias in ^{10}Be production reconstructed from ^{10}Be concentration is actually provided by the quantitative comparison with ^{14}C records.

4 Quantitative comparison of Beryllium-10 and radiocarbon

4.1 Carbon cycle model to compare both isotopes

Beryllium-10 and carbon-14 are both cosmogenic isotopes sensitive to solar activity. It has been shown (Siegenthaler and Beer 1988; Bard et al. 1997) that when ^{14}C production rate is reconstructed from ^{10}Be concentration, the generated ^{14}C variations compare quite well with ^{14}C variations measured in natural archives. This agreement is one of the best indications that ^{10}Be concentration is indeed a quantitative proxy of both ^{10}Be production and solar activity, despite potential biases due to ^{10}Be deposition (Sect. 3). Bard et al. (1997) and Horiuchi et al. (2008) have already shown that a good agreement hold for the South Pole and Dome Fuji ^{10}Be records. Here, we carry out this comparison for the stack of these records. We also test the impact of global carbon inventory in the models on the simulated atmospheric ^{14}C, a major source of uncertainty.

Both cosmogenic isotopes, ^{10}Be and ^{14}C, are produced in the atmosphere. However, a fundamental difference between them arises because ^{10}Be atoms are deposited very quickly after their production (within ~ 1 year; e.g., Raisbeck et al. 1981) whereas ^{14}C atoms are involved in the global carbon cycle in which they are 'diluted'. This 'dilution' attenuates and delays ^{14}C concentration variations in the different carbon reservoirs with respect to ^{14}C production variations. Moreover, the carbon cycle acts as a low pass filter because both attenuation and delay depend on the timescales of ^{14}C production variations (e.g., de Vries 1958; Stuiver 1961; Bard et al. 1997). This is shown by Fig. 1: atmospheric ^{14}C varies by $\sim 1\%$ whereas ^{10}Be concentrations vary by 10–30%. Also, ^{14}C peaks and troughs are delayed by few decades compared to their ^{10}Be counterparts. Thus, a quantitative comparison of ^{10}Be and ^{14}C concentrations requires to use a carbon cycle model. We use the ^{10}Be stack as a proxy of ^{14}C production to simulate atmospheric ^{14}C variations, and we compare these simulated ^{14}C variations with the reconstruction of IntCal04 (Reimer et al. 2004; Fig. 1). This 'direct' way of comparison between ^{10}Be and ^{14}C is different from the 'inverse' way by which the production of ^{14}C is inferred from the atmospheric ^{14}C content and compared with ^{10}Be concentration.

4.2 Reconstruction of ^{14}C production from ^{10}Be concentration

In order to estimate ^{14}C production, some corrections to ^{10}Be concentration must be applied. To a first order, productions of ^{14}C and ^{10}Be are equally sensitive to solar activity and geomagnetism due to similar production pathways, so that the ratio of both production rates is approximately constant, close to 110 (Masarik and Beer 1999). However, ^{10}Be concentration in Antarctic snow is more sensitive to solar activity and less to geomagnetism than atmospheric ^{14}C concentration. This arises for two reasons. First, the sensitivity of both production rates varies with latitude: their sensitivity to solar activity is much stronger at high latitudes than at low latitudes (about 50% more sensitive for a typical 11-year solar cycle), and conversely their sensitivity to geomagnetism is much stronger at low latitudes than at high latitudes (about twice less, e.g., Masarik and Beer 1999). Secondly, ^{14}C is well mixed in the atmosphere (its atmospheric concentration is thus sensitive to the global production), whereas ^{10}Be is quickly deposited onto the Antarctic surface (its snow concentration is more sensitive to the production at high latitudes). Hence we have to correct ^{10}Be concentration for this difference of sensitivity. The best way would be to combine contributions from different regions to the total flux of ^{10}Be deposited to the Antarctic surface, in order to calculate the average sensitivity to solar activity and geomagnetism. However, these contributions have not yet been estimated from observations. Hence we have to use modelling estimates of these sensitivities: Field et al. (2006) found that the polar flux of ^{10}Be is about 20% less sensitive to geomagnetism (and 20% more sensitive to solar activity) than the global production (and thus than the atmospheric concentration of ^{14}C). We use this result to correct ^{10}Be concentration and to estimate ^{14}C production.

This correction first accounts for changes in geomagnetic field. Since the deviation of galactic cosmic rays and the modulation of cosmogenic isotope production are mostly sensitive to the dipolar component of the geomagnetic field, we have to use a reconstruction of the virtual dipole moment (VDM). We use the recent reconstruction of Korte et al. (2009), which is based on spherical harmonics, the only approach able to isolate the VDM from other geomagnetic components of higher orders. Whatever the VDM reconstruction being used, the ^{10}Be production has to be increased by less than 4% over the last millennium (due to a stronger VDM), and the correction to get the ^{14}C production amounts to 20% of that increase (that is, less than $20\% \times 4\% = 0.8\%$). Hence, any uncertainty in the VDM corresponds to a very small uncertainty in the ^{14}C production. We use the sensitivity of Wagner et al. (2000) to calculate this geomagnetic correction, accounting for the small difference of sensitivity between ^{10}Be and ^{14}C production rates.

Once ^{10}Be concentration corrected for known geomagnetic changes, the residual must be corrected for the different sensitivities of ^{10}Be ice concentration and ^{14}C production rate to solar activity. This difference arises from two effects: (i) the ^{10}Be flux to polar regions is more

sensitive to solar activity (by about 20% according to Field et al. 2006, see above) than the global ^{10}Be production rate, and (ii) the global ^{14}C production rate is more sensitive (by 20–30% according to Masarik and Beer 1999) than the global ^{10}Be production rate. Given the strong uncertainty in the magnitude of the former sensitivity (from 20 to 40% according to Bard et al. 2000), we assume that both effects compensate, so that we do not further correct the ^{10}Be concentration residual and use it as a proxy of ^{14}C production to simulate atmospheric ^{14}C variations.

4.3 Carbon cycle models used to simulate ^{14}C variations

A range of global carbon cycle models exists, from simple box models to three dimensional ones. It is beyond the goal of this study to compare them: we restrict our study to two simple box models which are very close and differ only by their total quantity of carbon. Our goal is to show that some uncertainty in the simulated ^{14}C variations arises from the design of the model itself. As explained by Damon and Sternberg (1989), and Goslar (2001), the total quantity of carbon included in the model ('carbon inventory') affects the attenuation introduced by the model. A practical way to compare this effect is the so-called Bode diagram which represents, for sinusoidal variations in ^{14}C production, the attenuation factor (damping effect) as a function of the variation period (e.g., Houtermans 1966). This diagram is shown for three box models and for a zonally averaged model (Fig. 3). Characteristics of the models are given in Table 1.

The attenuation effect is such that variations of ^{14}C production are attenuated by a factor of about 100, 20, and 10 for decadal, centennial, and millennial variations, respectively (Fig. 3). Variations with a period longer than 10^5 years are almost not attenuated. This attenuation effect is slightly different between the models (within $\sim$30%). An obvious reason for this difference is the value of initial ^{14}C production (at a specific year or for mean pre-industrial conditions): this production is related to the model carbon inventory because ^{14}C production is inferred from the steady state assumption that it exactly compensates the decay of the total ^{14}C inventory. As explained by Damon and Sternberg (1989), and Goslar (2001), a model with a higher ^{14}C production has a more limited attenuation effect: for instance the 7 box model attenuates approximately 27% less than the 4 box model (for periods lower than 1,000 years, Fig. 3), a difference directly related to its 27% stronger ^{14}C production (Table 1). However, this relationship between ^{14}C production, carbon inventory, and attenuation is not simple: the 4 box and the Bern 2D models, for instance, have about the same carbon inventory but they differ in their attenuation. The relative size of carbon reservoirs, and the fluxes that are exchanged, are additional factors determining the attenuation in a carbon cycle model.

The other effect of the carbon cycle is to delay the response of atmospheric ^{14}C concentration with respect to variations in production. This delay is expressed in Fig. 3 as a phase lag. The phase lag ranges between 0 and 90°, with larger phase lag for shorter periods. Typically, for centennial variations the phase lag is about 45°, i.e., atmospheric ^{14}C concentration would lag the production by $\sim$12 years. This is precisely the lag between the South Pole ^{10}Be record and the IntCal04 ^{14}C record estimated by Bard et al. (1997) based on cross-correlation. The 12 box model accounts for a stratospheric production and predicts a phase lag larger than 90°, because the transfer time of ^{14}C to the troposphere adds up to the stratospheric phase lag of 90° (e.g., Siegenthaler et al. 1980). It is difficult to discuss this prediction, since adequate observations are lacking for that purpose. The time lag is actually less variable than the attenuation between the different models (see Table 1).

In the following, we discuss the results obtained with the 4 box and 7 box models, to illustrate the uncertainty in the reconstructed ^{14}C due to carbon inventory. These models have been chosen because the ratio of their attenuations is almost constant ($\sim$30%), and the phase lags are almost identical. The 12 box model attenuation is about 10% less than the 7 box model one at the decadal to centennial timescales, and their time lags are different by less than 3 years (Fig. 3).

4.4 Atmospheric carbon-14 variations calculated from the ^{10}Be time series

The ^{14}C production variations derived from the ^{10}Be stack (Sect. 4.2) are applied to the 4 box and the 7 box carbon cycle models. This allows us to simulate atmospheric ^{14}C concentration variations, starting approximately at year 700 AD or 840 AD depending on the Dome Fuji record chronology.

We have to keep carbon inventories and carbon fluxes constant during simulations since no reconstruction does exist. We thus assume that changes in the carbon cycle were limited enough to hardly affect ^{14}C (e.g., Marchal 2005) before the strong anthropogenic perturbations. This assumption is an important limitation of our exercise: for instance Stuiver and Braziunas (1993) argued that the difference between ^{10}Be-based and measured ^{14}C variations arise from climatic variations affecting the carbon cycle.

A practical problem with these simulations is to initialize radiocarbon inventories: because ^{14}C production has constantly changed, the ^{14}C cycle has clearly not been at steady state at any time in the past. Any difference with the

Table 1 Carbon cycle models used in this study (Figs. 3 and 4)

Name	Bern zonally averaged climate model	12 box model	7 box model	4 box model (7 box model without sediments)
Reference	Stocker and Wright (1996)	Bard et al. (1997)	Hughen et al. (2004)	Hughen et al. (2004)
Type of model	Dynamical model	Box model	Box model	Box model
Total carbon inventory [GtC]	41,700	43,800	57,000	41,800
Total ^{14}C inventory [10^6 mol]	3.3	3.8	4.6	3.6
Steady state ^{14}C production in moles/year and atom/cm^2/s	395/1.47	460/1.72	555/2.08	440/1.64
Attenuation factor and time lag for a 10-year production period	0.01/2 years	0.015/2 years	0.013/2 years	0.011/2 years
Attenuation factor and time lag for a 100-year production period	0.038/11 years	0.05/9 years	0.046/12 years	0.036/12 years
Attenuation factor and time lag for a 1,000-year production period	0.097/108 years	0.11/98 years	0.15/104 years	0.12/107 years

Carbon inventory is given in 10^{15} grams of carbon (GtC). The 4 box model is derived from the 7 box model of Hughen et al. (2004) by removing the sediments

real ^{14}C inventory at the beginning of a simulation propagates during the simulation (this difference actually decays with a half life of 5,730 years). We addressed this problem by starting the simulations at year 500 BC, i.e., more than 1,000 years before the beginning of the production time series. For this, we inferred a ^{14}C production from the IntCal04 record over the last 2,500 years (following, e.g., Stuiver and Quay 1980), and substituted its latest part with the ^{10}Be-derived production. At the start of the ^{10}Be-derived production (approximately year 700 AD or 840 AD), the model ^{14}C inventory is expected to be more realistic than the steady state ^{14}C inventory. On the other hand, both production series are not perfectly consistent with each other, so a perfect match between simulated and reconstructed atmospheric ^{14}C is not expected.

Figure 4 compares atmospheric ^{14}C concentration variations simulated with the production time series based on the three different chronologies of the Dome Fuji ^{10}Be record (Sect. 4.2), with the IntCal04 atmospheric ^{14}C variations. The chronologies based only on volcanic stratigraphy (top and bottom of Fig. 4) are independent of the IntCal04 reconstruction, whereas the chronology adjusted to ^{14}C (middle of Fig. 4) is not completely independent. As noticed by Siegenthaler and Beer (1988), Bard et al. (1997) and Horiuchi et al. (2008), a good match is found between simulated and measured atmospheric ^{14}C variations, both in amplitude and phase. The correlation coefficients are very high, with r^2 close to 0.9 (Table 2), suggesting that ^{10}Be concentration in Antarctic ice is a quantitative proxy of cosmogenic isotope production. Because the initial ^{14}C inventory of the model is not very accurate, there is a slight and almost constant shift in the simulated ^{14}C atmospheric concentrations compared to the IntCal04 ones (less than 10 permil), so that the simulated curves have been shifted up in Fig. 4 for a better comparison. The concentrations of atmospheric ^{14}C are expressed in $\Delta^{14}C$ units, i.e., as relative variations with respect to the standard reference value (Stuiver and Polach 1977).

Whereas the peaks and troughs are quite in phase, there is not a perfect match between the simulated and IntCal04 $\Delta^{14}C$ variations. Important differences are found during two periods ranging (i) from approximately year AD 1150 to year AD 1450 with $\Delta^{14}C$ levels too low on average by $\sim$5‰ with the 4 box model and by $\sim$7‰ with the 7 box model (with differences up to 10 and 13‰, respectively); and (ii) from approximately year AD 1450 to year AD 1720 with $\Delta^{14}C$ levels too high on average by $\sim$3‰ with the 4 box model and by $\sim$7‰ with the 7 box model (with differences up to 10 and 13‰, respectively). The low $\Delta^{14}C$ levels simulated during the 12th to 15th centuries are mostly due to low values in the South Pole ^{10}Be record, including one very low value around year 1134 AD, except during the 1128–1160 AD period during which both South Pole and Dome Fuji ^{10}Be records have low values. The high $\Delta^{14}C$ levels simulated between the Spörer and the Maunder Minima are mostly due to high values of the Dome Fuji ^{10}Be record, except at the end of the Spörer Minimum when they are due to high values of the South Pole ^{10}Be record, although the Dome Fuji record features a secondary peak which also contributes to this high level (between approximately years 1570 and 1600 AD, Fig. 1).

We have also tried to compare the amplitude of the main $\Delta^{14}C$ peaks, corresponding to solar minima, although it is difficult to define the bounds of such aperiodic variations. The results are compiled in Table 3. The amplitudes simulated by the 7 box model are 27 ± 1% larger than their counterparts simulated with the 4 box model, in agreement with the 27% difference expected from the attenuation

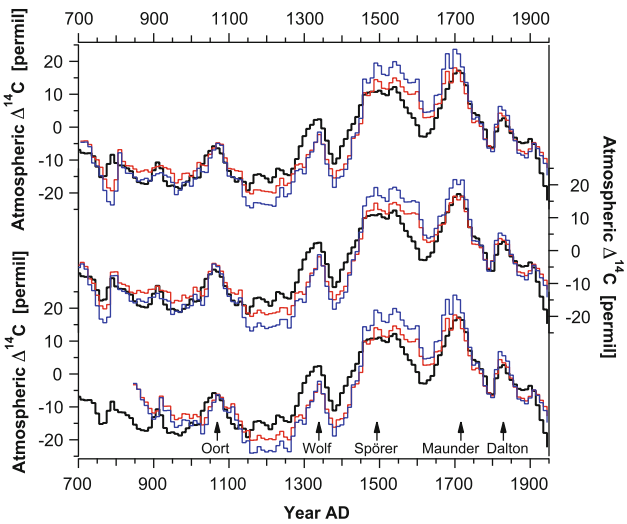

Fig. 4 Relative variations in atmospheric ^{14}C content simulated by applying the ^{10}Be-based ^{14}C production dated with three different chronologies for the Dome Fuji record (*top*: initial chronology based on 5 volcanic eruptions; *middle*: these 5 eruptions plus adjustment to ^{14}C; *bottom*: 3 additional eruptions) to two different models (4 box model in *red*; 7 box model in *blue*), compared to the northern hemisphere reconstruction by IntCal04 in *black*. The simulated variations have been shifted vertically (by 7–10 permil) to match the average of the IntCal04 values over the same period. All curves are 10-year averages, which corresponds approximately to the original ^{10}Be concentration resolution. The major solar Minima are labeled

factor for centennial variations (Table 1). In general, the simulated $\Delta^{14}C$ amplitudes agree with the IntCal04 ones within 2–3‰. A poorer agreement is found for the $\Delta^{14}C$ increases at the beginning of the Spörer and Maunder Minima, with differences up to 8‰ with the 4 box model and 14‰ with the 7 box model.

This general agreement between simulated and the IntCal04 ^{14}C variations is remarkable when compared to the uncertainty in ^{14}C production: in particular the expected bias due to variations in snow accumulation (up to 15% over a century, see Sect. 3.3) would translate into 8‰ of systematic bias between simulated and real $\Delta^{14}C$ variations. Such a bias is hardly found to persist over such a long time (Fig. 4), with two exceptions: over the end of the Spörer Minimum, and over both periods detailed above (1150–1450 AD and 1450–1750 AD) but only for the 7 box model simulated values. This small difference of few permils between the simulated and IntCal04 $\Delta^{14}C$ variations suggests that the bias in ^{10}Be production may be limited to 10% at the centennial timescale, instead of 15% as inferred from potential accumulation change (Sect. 3.3). Also, it is probably close to the uncertainty of the IntCal04 $\Delta^{14}C$ as proxy of ^{14}C production, because atmospheric ^{14}C content may have been additionally affected by small variations in the carbon cycle (e.g., Stuiver and Braziunas 1993).

Based on Fig. 4 and Table 2, the 4 box model simulates $\Delta^{14}C$ variations which best match the IntCal04 variations, in terms of amplitude. The $\Delta^{14}C$ variations simulated with the Bern 2D model are intermediate between those simulated with the 4 and 7 box models (not shown). Hence, provided that the polar enhancement of the ^{10}Be flux is only 20% as found by Field et al. (2006), this comparison between simulated and reconstructed $\Delta^{14}C$ suggests that a model with small carbon inventory and ^{14}C production is more realistic.

Overall, the best match between simulated and IntCal04 $\Delta^{14}C$ reconstructions is obtained by using the stacked and Dome Fuji ^{10}Be records ($r^2 \approx 0.9$, compared to ~ 0.6 with the South Pole ^{10}Be record). Provided, again, that atmospheric ^{14}C concentration is a better proxy of ^{14}C production than ^{10}Be concentration, this suggests that the stacked ^{10}Be record is as good as the Dome Fuji one, and better than the South Pole one, as proxy of solar variability.

The high level of correlation between ^{10}Be and ^{14}C variations ($r^2 \approx 0.9$) also suggests that any improvement of this correlation is difficult to expect: both isotope records are very different in nature and require several corrections to be compared.

5 Reconstruction of solar activity from the Antarctic ^{10}Be stack

5.1 Modulation of ^{10}Be production by the solar open magnetic flux

Stacking both Antarctic ^{10}Be records provides us with a long record spanning the industrial period (approximately

Table 2 Determination coefficients (r^2) between the atmospheric ^{14}C concentration variations reconstructed by IntCal04 and simulated with the different models and chronologies (Fig. 4), with a 10-year time resolution, calculated between the beginning of the record and year 1900 AD

Chronology of the Dome Fuji record/carbon model	5 volcanic eruptions of Horiuchi et al.	5 volcanic eruptions + adjustment to ^{14}C production	8 volcanic eruptions
4 box model	0.86 ($n = 121$)	0.87 ($n = 121$)	0.80 ($n = 107$)
7 box model	0.87 ($n = 121$)	0.87 ($n = 121$)	0.80 ($n = 107$)

With the first two chronologies, the stack starts at about year 700 AD, whereas with the last chronology the stack starts at about year 840 AD. All determination coefficients are significant with $p < 0.0001$

Table 3 Comparison of atmospheric ^{14}C concentration variations corresponding to ^{14}C peaks (solar minima) between the simulated and the IntCal04 (Reimer et al. 2004) variations

Atmospheric ^{14}C peaks	^{14}C minima before and after peak (year AD)	^{14}C peak (year AD)	simulated ^{14}C amplitudes (‰)	IntCal04 ^{14}C amplitudes (‰)
Oort Minimum	1015; 1115	1055	8.5; −9.4 (4 box)	9.5; −10.8
			10.8; −11.9 (7 box)	
Wolf Minimum	1255; 1375	1335	17.6; −13 (4 box)	17.0; −13.5
			22.3; −16.6 (7 box)	
Spörer Minimum	1375; 1615	1535	29.5; −11.4 (4 box)	23.3; −15.1
			37.1; −14.6 (7 box)	
Maunder Minimum	1615; 1785	1705	12.2; −20.8 (4 box)	20.1; −23.0
			15.4; −26.3 (7 box)	
Dalton Minimum	1785; 1875	1825	8.5; −9.9 (4 box)	8.5; −7.6
			10.9; −12.5 (7 box)	

Only the simulated ^{14}C variations using the ^{14}C-adjusted chronology for the production are considered here. Two values are given, corresponding to the increase and the decrease before and after each peak, respectively. Values and years are taken from the 10-year averaged data

to year 1980 AD). This allows us to calibrate this ^{10}Be stack using solar activity measurements, and to propose a quantitative reconstruction of solar activity over the last millennium. The comparison of this reconstruction with ones independent of cosmogenic isotopes is the only way to test our hypothesis that the stacking procedure has removed part of the non-solar variability. We use in the following the ^{10}Be stack based on the ^{14}C-adjusted chronology of the Dome Fuji record, because this chronology seems to be more realistic (especially before year 1260 AD) than the chronology based only on volcanic eruptions.

The ^{10}Be production is mainly due to the flux of galactic cosmic rays (GCR). This flux is modulated by the interplanetary magnetic field, which is mainly composed of the heliospheric open magnetic flux. In contrast, variations of TSI are physically related to the photospheric closed magnetic flux (e.g., Wang et al. 2000). Linear correlations have been proposed between the open magnetic flux (measured with the *Aa* index, cosmic ray flux, and cosmogenic isotopes) and TSI over the last decades (Lockwood and Stamper 1999; Lockwood 2002; Fröhlich 2009). But over the last centuries, the relationship between the open magnetic flux and TSI appears to be non linear (Mursula et al. 2003). So far, it seems difficult to estimate a centennial trend in TSI without assuming a particular TSI level during quiet solar phase like the Maunder Minimum.

On the other hand, physical models are able to simulate various quantities related to the open magnetic flux: the modulation parameter, sunspot number, GCR, and cosmogenic isotope production (e.g., Usoskin et al. 2002). Hence, assuming that the Antarctic ^{10}Be stack does reliably represent variations of cosmogenic isotope production, we use the stack to reconstruct the modulation parameter (or potential) Φ. This modulation parameter quantifies the deceleration of GCR due to solar activity (Gleeson and Axford 1968). Its expected lower bound is zero, which corresponds to the absence of solar modulation and to the full local interstellar GCR flux. The energy spectrum of this GCR flux (so-called Local Interstellar Spectrum, LIS) is required in order to estimate the sensitivity of the cosmogenic production to the modulation parameter. The LIS is not well known, which introduces some uncertainty when relating cosmogenic production to solar activity.

5.2 Calibration to modulation parameter measurements

To reconstruct the modulation parameter Φ, the ^{10}Be stack is first corrected for the geomagnetic field by using the recent reconstruction of Korte et al. (2009) (as described in Sect. 4.2), although this is a small correction (Bard et al. 2007). We follow the method of McCracken et al. (2004), which has been already applied to the South Pole record, assuming an average level for Φ of 645 MV over the 22-year period of years 1946–1969 AD, and using the LIS and the sensitivity of ^{10}Be production to modulation parameter calculated by Webber and Higbie (2003). We underline that our reconstruction of Φ is sensitive to this assumed average level of Φ, particularly because the most recent part of the ^{10}Be stack is only comprised of the South Pole record. Due to the discontinuous sampling of the South Pole ice core, the 22-year period closest to years 1946–1969 AD is 1944–1966 AD. The average value of the ^{10}Be stack over this period is set to 645 MV which allows us to scale the rest of the stack.

5.3 Sensitivity to the geographical origin of ^{10}Be

The geographical origin of ^{10}Be deposited to Central Antarctica has to be accounted for (Sect. 4.2), as it introduces the main uncertainty in the modulation parameter

reconstruction. In fact, cosmogenic isotope production is more sensitive to the modulation parameter at high than at low latitudes (by a factor ~2, e.g., Masarik and Beer 1999). Hence, assuming that the ^{10}Be deposited in Central Antarctica is entirely produced at high latitudes would result in the smallest changes in the modulation parameter Φ. The stronger the contribution of lower latitudes to the Antarctic flux of ^{10}Be, the stronger the inferred changes in Φ. McCracken et al. (2004) used a moderate contribution from the lowest latitudes to the South Pole ^{10}Be flux: their mixing model "M3" implies that relative variations of the global ^{10}Be production are attenuated by a factor 0.65 compared to relative variations in polar regions. This corresponds to a polar enhancement coefficient (PEC) of 0.65 following the definition of Bard et al. (1997). Here, we calculate the modulation parameter Φ for two cases: (i) the lower bound case which assumes that all ^{10}Be is produced at high latitudes (i.e., poleward of ~60°S, corresponding to a PEC of ~0.5), and (ii) a more realistic case which assumes an important contribution of ^{10}Be from middle latitudes (40°S, PEC of ~0.8). This latter source at 40°S has been chosen because the production rate of ^{10}Be at this latitude approximately corresponds to the global production rate. The respective contribution of both sources (high latitudes and 40°S) is calculated by combining two information. In their modelling work, Field et al. (2006) decrease the modulation parameter from 700 to 500 MV: they show that an increase by 10% of the global ^{10}Be production translates into an increase by 12.4% of ^{10}Be flux in polar regions, which corresponds to a PEC of 0.76. Further, calculations by Webber and Higbie (2003) show that the ^{10}Be production increase due to the same modulation parameter decrease (700–500 MV) is about 20% at high latitudes (>60°), and 9% at middle latitudes (40°). Hence, the 12.4% increase in ^{10}Be flux found by Field et al. (2006) can be simply explained by contributions of 31% from the high latitudes and 69% from the middle latitudes (i.e., $0.31 \times 20\% + 0.69 \times 9\% = 12.4\%$). We use this mixing model with constant contributions from two sources, much simpler than the one used by McCracken et al. (2004).

5.4 Reconstructed solar modulation parameter

Variations of the modulation parameter Φ are shown in Fig. 5 for both mixing cases. The modulation parameter shows a general trend of a solar activity decrease from the 8th century to the 15th century, followed by an increase, a trend already shown by different proxies (e.g., Stuiver and Quay 1980). The difference between the maxima is smaller (~100–200 MV) than between the minima (up to 400 MV). The lowest value corresponds to the Spörer Minimum with values roughly between 150 and 0 MV. Four

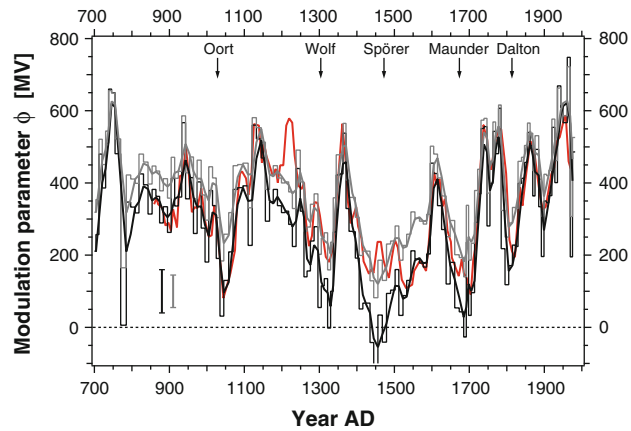

Fig. 5 Solar modulation parameter Φ estimated from the Antarctic ^{10}Be stack using the ^{14}C adjusted chronology (Fig. 1), assuming a purely local production (*grey lines*) or a 70% contribution from the middle latitudes (*black lines*). *Bold lines* are smoothed versions with a 1-2-1 box filter, to facilitate comparison with previous estimates. *Error bars* show the typical 1σ uncertainty accounting for (i) the analytical precision of the ^{10}Be concentration measurements and (ii) the bias due to snow accumulation variations. The *red curve* is the estimate by McCracken et al. (2004) based on the South Pole ^{10}Be record only

values are found to be negative, three during the Spörer Minimum and one during Maunder Minimum, although only one (at year 1456 AD) is significant given the 2σ uncertainty in ^{10}Be measurements. A negative value of Φ corresponds to a ^{10}Be production stronger than the maximum production due to the non-modulated, full GCR flux. McCracken et al. (2004) also obtained a negative value during this period from the South Pole ^{10}Be record (this value is removed from the curve in Fig. 5). They attributed this negative value to a burst of cosmic rays from the Sun or a supernova. By using records of recent solar proton events, Usoskin et al. (2006a) and Webber et al. (2007) have shown that ^{10}Be production may have been increased by 50% during these events. In our ^{10}Be records, such a 50% increase would have been averaged over the time covered by an ice sample, that is, between 4 and 8 years: this leaves us with a 5–10% increase. This increase is strong enough to shift the negative value found around year 1456 AD to a positive value. Other possibilities independent of solar activity could explain negative Φ values, like a rapid decrease in snow accumulation or a change in LIS.

5.5 Comparison with the South Pole reconstruction of McCracken et al

Our reconstruction of Φ based on the stacked records and a constant mixing scheme compares quite well with the one of McCracken et al. (2004) based on the South Pole record and their mixing model "M3" (Fig. 5), with three marked differences. First, the Spörer Minimum corresponds to the

weakest activity in our reconstruction, even after removing the lowest values around year 1456 AD. Another important difference is a secondary maximum centered around year 1220 AD in the South Pole reconstruction, which does not exist at all in our stack. A third important difference concerns the rank of the minima: in our stack the Spörer is the lowest minimum, followed by the Maunder, Wolf, Oort, and Dalton Minima, that is, the Oort and Maunder Minima are higher than in the McCracken et al. reconstruction. The maximum of Φ is found during the 20th century based on the raw Φ values, but during the 8th century based on smoothed Φ values. In this perspective, the recent centennial solar activity is not stronger than over the past 1,300 years, contrary to what has been proposed by Solanki et al. (2004), and in line with results discussed by Muscheler et al. (2007) and Bard et al. (2007).

As discussed in Sect. 3.3, trends in snow accumulation have probably biased the relative values of Φ, and this would affect the rank of the reconstructed solar Minima and maxima. In particular, the expected decrease in snow accumulation during the 16th and 17th centuries would have increased ^{10}Be concentration and biased Φ towards lower values. However, this bias would not (or less) apply to our reconstructed Spörer Minimum and would even lower the Maunder Minimum. Based on probable accumulation trend (Sect. 3.2) and on the comparison between simulated and IntCal04 ^{14}C variations (Sect. 4.4), we could bound the bias in ^{10}Be concentration to 10–15%. To test the robustness of the Spörer Minimum, we account for the upper level of uncertainty (worst case) by decreasing ^{10}Be production by 15% to account for a possible lower accumulation over the period 1440–1480 AD, and by 25% at year 1456 AD to account for a possible additional contribution of solar proton event: the smoothed Spörer Minimum is then at the same level than the Maunder Minimum. This is the 'worst case' since the possible bias of accumulation would also lower the Maunder Minimum. Thus, our results suggest that the Spörer Minimum is as low or even lower than the Maunder Minimum.

Similarly, the expected increase in snow accumulation during the last three centuries would have decreased ^{10}Be concentration and biased Φ towards higher values. A 5% increase in snow accumulation during the recent years (Sect. 3.2) would have increased Φ by 50 MV. Such a bias to higher values of Φ reinforces the conclusion that the solar activity maximum during the 20th century is not exceptionally strong over the last millennium.

5.6 Comparison with other reconstructions

Usoskin et al. (2005) have compared five estimates of the modulation parameter over the last 50 years, each based on a particular approximation of LIS. The one by Webber and Higbie (2003), on which our calculations are based, gives the lowest values of the modulation parameter Φ. Usoskin et al. (2005) found that, to a first order, the five estimates of Φ are linearly related (see their Appendix A4), with a maximum difference of about 200 MV. These linear relationships allow us to compare our reconstructions of the modulation parameter Φ with other ones compiled and scaled to the same LIS approximation by Usoskin et al. (2006b) (their Fig. 1). Our reconstructions of Φ are in the highest part of the range, especially during the Maunder Minimum and over the second part of the 20th century. More specifically, compared to the reconstructions by Muscheler et al. (2005) and Muscheler et al. (2007), based on ^{14}C and ^{10}Be records, our reconstruction has a much lower variability and lower maxima values. Especially, peaks around years 1120, 1600, 1780, and 1960 AD are not found or not as high as in the Muscheler et al. reconstructions. Also, their 20th century maximum is considerably higher by few hundreds of MV (except the year ~1780 AD peak) than the other maxima, which is not the case in our reconstructions. These features have already been stressed by Solanki et al. (2005) and Bard et al. (2007), which point out possible problems in the calibration and/or in stacking ^{10}Be records from both Greenland and Antarctic sites. These sites are very different in terms of accumulation, climatic trend, and probably geographical origin of ^{10}Be. By contrast, the two sites used in this study have some similarities, in terms of deposition mode, and probably geographical origin of ^{10}Be, which makes the stack more consistent. Both modelling studies of Field and Schmidt (2009) and Heikkilä et al. (2008) suggest a stronger spatial variability of ^{10}Be flux and a stronger climatic impact on ^{10}Be concentration in Greenland compared to Central Antarctica (although accumulation is not well simulated in the latter region).

5.7 Conversion into TSI

Conversion of solar activity into total solar irradiance is not straightforward, for at least two reasons: (i) the very short period of direct TSI measurements (~30 years) does not allow a precise calibration, and (ii) the observed relationship between Φ and TSI may have been different during solar quiet periods. Still, we provide a TSI reconstruction as a practical means to test our reconstruction of solar activity, especially as a forcing in climatic models. We base the TSI calculation on the assumption of a 0.08% increase from the Maunder Minimum to an averaged modern maximum of 1,365.5 W/m^2. This increase corresponds to the 'most likely' value of 0.04% proposed in IPCC AR4 (IPCC 2007, p. 192), augmented by the effect of averaging the modern 11-year cycles (see note a of Table 2.10 in IPCC AR4). This assumption completely

defines the amplitude of TSI, regardless of the amplitude of the solar modulation parameter. This makes our TSI reconstruction independent of the ^{10}Be geographical origin (PEC value). We use the smoothed modulation parameter reconstruction of Fig. 5 in order to completely remove the 11-year solar cycle. The reconstructed TSI is available as supplemental data.

6 Conclusion

We propose a new reconstruction of solar modulation parameter Φ over the period of years ~700 AD to ~1980 AD, based on a stack of two ^{10}Be concentration records from Central Antarctica. Stacking these records together has two advantages: (i) to remove part of the subdecadal variability of deposition and snow accumulation, uncorrelated between both sites and unrelated to solar activity; and (ii) to extend the period of time covered by ^{10}Be, allowing us to calibrate this record with direct measurements of solar activity.

Although Central Antarctica offers favorable conditions to record solar activity, the data required to control the validity of ^{10}Be as a proxy of solar activity are scarce. In contrast to previous studies, we have tried to estimate the three main uncertainties on this proxy. First, the relationships between ^{10}Be or sulfate concentrations and accumulation suggest that dry deposition has been dominating the flux of ^{10}Be to both Antarctic sites. The proportion of dry deposition can be combined with an estimate of snow accumulation variations to infer an upper limit of 10–15% to the systematic bias in solar activity due to accumulation. Independently, the comparison of ^{10}Be variations with reconstructed atmospheric ^{14}C variations suggests a maximum bias of 10%. Second, the dating of the Dome Fuji ^{10}Be record is based on a loose volcanic stratigraphy which has been refined by adjustments to ^{14}C variations: this seems justified given the very strong correlation between these adjusted ^{10}Be variations and both the South Pole ^{10}Be variations and atmospheric ^{14}C variations. This dating refinement considerably decreases the dating uncertainty in the stack to approximately 10 years. Third, a remaining large source of uncertainty is the geographical origin of ^{10}Be deposited to Antarctica, which affects the amplitude of solar activity reconstructed from the ^{10}Be variations. We consider two extreme cases for this origin, which lead to two different reconstructions of solar activity, quantified with the solar modulation parameter Φ.

The minima of the solar modulation parameter are found to be much more variable than the maxima, with the Spörer Minimum being the lowest of them. At the centennial timescale, the maximum of the 20th century is lower than the one of the 8th century. This reinforces the conclusion made previously (e.g., Muscheler et al. 2007; Bard et al. 2007) that the current solar activity is not exceptionally high over the last millennium. A TSI reconstruction is also provided as a means to test our solar activity reconstruction.

The limitations and uncertainties of our reconstructions of Φ and TSI must be stressed, most importantly: (i) the ^{10}Be records of South Pole and Dome Fuji present some unresolved discrepancies, especially during the 16th century; (ii) both reconstructions of Φ and TSI entirely rely on a calibration of the sole South Pole record over the last decades; and (iii) the geographical origin of ^{10}Be remains a major source of uncertainty for the amplitude of the reconstructed series. Still, we hope this study will help clarify advantages and drawbacks of Antarctic ^{10}Be records, and will contribute to a better understanding of solar activity over the last millennium. Further comparisons with independent and new records of solar activity, especially ^{10}Be records from high latitudes, are required to test its significance.

Beryllium-10 stack and solar activity reconstructions are provided as supplementary materials as well as on the NCDC/Paleo web site.

Acknowledgments We are indebted to Dr. Horiuchi for providing us the Dome Fuji ^{10}Be data and for some comments, and to the reviewers for their constructive comments and careful language corrections. This study is a contribution to the VOLSOL project (ANR-09-BLAN-0003-01) funded by Agence Nationale de la Recherche (ANR).

References

Bard E et al (1997) Solar modulation of cosmogenic nuclide production over the last millennium: comparison between ^{14}C and ^{10}Be records. Earth Planet Sci Lett. doi:10.1016/S0012-821X(97)00082-4

Bard E et al (2000) Solar irradiance during the last 1200 years based on cosmogenic nuclides. Tellus. doi:10.1034/j.1600-0889.2000.d01-7.x

Bard E et al (2007) Comment on "Solar activity during the last 1000 yr inferred from radionuclide records" by Muscheler et al. (2007). Quat Sci Rev. doi:10.1016/j.quascirev.2007.06.002

Beer J et al (1987) ^{10}Be measurements on polar ice: comparison of Arctic and Antarctic records. Nucl Instrum Methods Phys Res B 29:203–206. doi:10.1016/0168-583X(87)90236-9

Beer J et al (1990) Use of ^{10}Be in polar ice to trace the 11-year cycle of solar activity. Nature. doi:10.1038/347164a0

Beer J, Tobias S, Weiss N (1998) An active sun throughout the Maunder Minimum. Solar Phys. doi:10.1023/A:1005026001784

Berggren A-M et al (2009) A 600-year annual ^{10}Be record from the NGRIP ice core, Greenland. Geophys Res Lett 36:L11801. doi:10.1029/2009GL038004

Bergin MH et al (1998) Relationship between continuous aerosol measurements and firn core chemistry over a 10-year period at the South Pole. Geophys Res Lett 25:1189–1192. doi:10.1029/98GL00854

Damon PE, Sternberg RE (1989) Global production and decay of radiocarbon. Radiocarbon 31:697–703

de Vries HL (1958) Variation in concentration of radiocarbon with time and location on earth. Proc Koninklijke Nederlandse Akademie van Wetenschappen B61:94–102

Delmas RJ (1992) Free tropospheric reservoir of natural sulfate. J Atmos Chem. doi:10.1007/BF00115238

Delmas RJ et al (1992) 1000 years of explosive volcanism recorded at the South Pole. Tellus. doi:10.1034/j.1600-0889.1992.00011.x

Ekaykin AA et al (2002) Spatial and temporal variability in isotope composition of recent snow in the vicinity of Vostok station, Antarctica: implications for ice-core record interpretation. Ann Glaciol 35:181–186. doi:10.3189/172756402781816726

Ekaykin AA et al (2004) The changes in isotope composition and accumulation of snow at Vostok station, East Antarctica, over the past 200 years. Ann Glaciol. doi:10.3189/172756404781814348

Field CV et al (2006) Modeling production and climate-related impacts on ^{10}Be concentration in ice cores. J Geophys Res. doi:10.1029/2005JD006410

Field CV, Schmidt GA (2009) Model-based constraints on interpreting 20th century trends in ice core ^{10}Be. J Geophys Res. doi:10.1029/2008JD011217

Fröhlich C (2009) Evidence of a long-term trend in total solar irradiance. Astron Astrophys. doi:10.1051/0004-6361/200912318

Gleeson LJ, Axford WI (1968) Solar modulation of galactic cosmic rays. Astrophys J 154:1011–1026

Goslar T (2001) Absolute production of radiocarbon and the long-term trend of atmospheric radiocarbon. Radiocarbon 43:743–749

Hansen J et al (2008) Target atmospheric CO_2: where should humanity aim? Open Atmos Sci J 2:217–231. doi:10.2174/1874282300802010217

Harder S, Warren SG, Charlson RJ (2000) Sulfate in air and snow at the South Pole: implications for transport and deposition at sites with low snow accumulation. J Geophys Res. doi:10.1029/2000JD900351

Heikkilä U, Beer J, Feichter J (2008) Modeling cosmogenic radionuclides ^{10}Be and ^{7}Be during the Maunder Minimum using the ECHAM5-HAM General Circulation Model. Atmos Chem Phys 8:2797–2809

Heikkilä U, Beer J, Feichter J (2009) Meridional transport and deposition of atmospheric ^{10}Be. Atmos Chem Phys 9:515–527

Horiuchi K et al (2007) Concentration of ^{10}Be in an ice core from the Dome Fuji station, Eastern Antarctica: preliminary results from 1500 to 1810 yr AD. Nucl Instrum Methods Phys Res. doi:10.1016/j.nimb.2007.01.306

Horiuchi K et al (2008) Ice core record of ^{10}Be over the past millennium from Dome Fuji, Antarctica: a new proxy record of past solar activity and a powerful tool for stratigraphic dating. Quatern Geochronol. doi:10.1016/j.quageo.2008.01.003

Houtermans JC (1966) On the quantitative relationships between geophysical parameters and the natural C14 inventory. Zeitschrift für Physik 193:1–12

Hughen K et al (2004) ^{14}C activity and global carbon cycle changes over the past 50,000 years. Science 303:202–207

Huke M et al (2002) Air-firn-transfer of ^{10}Be at European deep drilling sites in Antarctica. Paul Scherrer Institute Annual report, Villigen, Switzerland

Iizuka Y et al (2004) SO_4^{2-} minimum in summer snow layer at Dome Fuji, Antarctica, and the probable mechanism. J Geophys Res 109:D04307. doi:10.1029/2003JD004138

IPCC (2007) Climate Change 2007 - The Physical Science Basis. Cambridge University Press, Cambridge, UK

Joussaume S, Taylor KE (1995) Status of the paleoclimate modeling intercomparison project (PMIP). In: Gates WL (ed) Proc First Int AMIP Sci Conf, Monterey, pp 425–430

Jouzel J et al (1983) Climatic information over the last century deduced from a detailed isotopic record in the South Pole snow. J Geophys Res. doi:10.1029/JC088iC04p02693

Kameda T et al (1997) Surface mass balance, sublimation and snow temperatures at Dome Fuji Station, Antarctica, in 1995. Proc 19th NIPR Symp Polar Meteorol Glaciol 11:24–34

Kameda T et al (2008) Temporal and spatial variability of surface mass balance at Dome Fuji, East Antarctica, by the stake method from 1995 to 2006. J Glaciol. doi:10.3189/002214308784409062

Kirchner S, Delmas RJ (1988) A 1000 year glaciochemical study at the South Pole. Ann Glaciol 10:80–84

Korte M, Donadini F, Constable CG (2009) Geomagnetic field for 0–3 ka: 2. A new series of time-varying global models. Geochem Geophys Geosyst. doi:10.1029/2008GC002297

Legrand M (1987) Chemistry of Antarctic snow and ice. J Physique 48(suppl):78–86

Legrand M (1995) Sulphur-derived species in polar ice: a review. In: Delmas RJ (ed) Ice core studies of global biogeochemical cycles. Springer, Berlin, pp 91–119

Lockwood M, Stamper R (1999) Long-term drift of the coronal source magnetic flux and the total solar irradiance. Geophys Res Lett. doi:10.1029/1999GL900485

Lockwood M (2002) An evaluation of the correlation between open solar flux and total solar irradiance. Astron Astrophys. doi:10.1051/0004-6361:20011666

Marchal O (2005) Optimal estimation of atmospheric ^{14}C production over the Holocene: paleoclimate implications. Clim Dyn. doi:10.1007/s00382-004-0476-z

Masarik J, Beer J (1999) Simulation of particle fluxes and cosmogenic nuclide production in the Earth's atmosphere. J Geophys Res 104:12099–12111

Masson V et al (2000) Holocene climate variability in Antarctica based on 11 ice-core isotopic records. Quatern Res. doi:10.1006/qres.2000.2172

McCracken KG (2004) Geomagnetic and atmospheric effects upon the cosmogenic ^{10}Be observed in polar ice. J Geophys Res. doi:10.1029/2003JA010060

McCracken KG et al (2004) A phenomenological study of the long-term cosmic ray modulation, 850–1958 AD. J Geophys Res. doi:10.1029/2004JA010685

Mosley-Thompson E et al (1999) Late 20th Century increase in South Pole snow accumulation. J Geophys Res. doi:10.1029/1998JD200092

Mursula K, Usoskin IG, Kovaltsov GA (2003) Reconstructing the long-term cosmic ray intensity: Linear relations do not work. Ann Geophys 21:863–867

Muscheler R et al (2005) Climate: how unusual is today's solar activity? Nature. doi:10.1038/nature04045

Muscheler R et al (2007) Solar activity during the last 1000 yr inferred from radionuclide records. Quat Sci Rev. doi:10.1016/j.quascirev.2006.07.012

Narita H et al (2003) Estimation of annual layer thickness from stratigraphical analysis of Dome Fuji deep ice core. Mem Natl Inst Polar Res 57(Special issue):38–45

Pedro J et al (2006) Evidence for climate modulation of the ^{10}Be solar activity proxy. J Geophys Res. doi:10.1029/2005JD006764

Raisbeck GM et al (1981) Cosmogenic ^{10}Be/^{7}Be as a probe of atmospheric transport processes. Geophys Res Lett 8:1015–1018. doi:10.1029/GL008i009p01015

Raisbeck GM, Yiou F (1985) ^{10}Be in polar ice and atmospheres. Ann Glaciol 7:138–140

Raisbeck GM et al (1990) ^{10}Be and δ^2H in polar ice cores as a probe of the solar variability's influence on climate. Philos Trans Royal Soc London. doi:10.1098/rsta.1990.0027

Reimer PJ et al (2004) IntCal04 terrestrial radiocarbon age calibration, 0–26 Cal Kyr BP. Radiocarbon 46:1029–1058

Satow K et al (1999) The relationship among accumulation rate, stable isotope ratio and surface temperature on the plateau of East Dronning Maud Land, Antarctica. Polar Meteorol Glaciol 13:43–52

Shaw GE (1988) Antarctic aerosols: a review. Rev Geophys 26:89–112

Shindell DT et al (2003) Volcanic and solar forcing of climate change during the preindustrial era. J Climate. doi:10.1175/1520-0442(2003)016<4094:VASFOC>2.0.CO;2

Siegenthaler U, Beer J (1988) Model comparison of ^{14}C and ^{10}Be Isotope records. In: Stephenson FR, Wolfendale AW (eds) Secular solar and geomagnetic variations in the last 10,000 years. Kluwer, Durham, pp 315–328

Siegenthaler U, Heimann M, Oeschger H (1980) ^{14}C variations caused by changes in the global carbon cycle. Radiocarbon 22:177–191

Smith AM et al (2000) ^{7}Be and ^{10}Be concentrations in recent firn and ice at Law Dome, Antarctica. Nucl Instrum Methods Phys Res B. doi:10.1016/S0168-583X(00)00281-0

Solanki SK et al (2004) Unusual activity of the Sun during recent decades compared to the previous 11,000 years. Nature. doi:10.1038/nature02995

Solanki SK et al (2005) Climate: how unusual is today's solar activity? (reply). Nature. doi:10.1038/nature04046

Steig E, Stuiver M, Polissar P (1995) Cosmogenic isotope concentrations at Taylor Dome, Antarctica. Antarct. J. U. S. 30:95–97

Stocker TF, Wright DG (1996) Rapid changes in ocean circulation and atmospheric radiocarbon. Paleoceanography. doi:10.1029/96PA02640

Stuiver M (1961) Variations in radiocarbon concentration and sunspot activity. J Geophys Res 66:273–276

Stuiver M, Polach HA (1977) Discussion: reporting of ^{14}C data. Radiocarbon 19:355–363

Stuiver M, Quay PD (1980) Changes in atmospheric carbon-14 attributed to a variable sun. Science 207:11–19

Stuiver M, Braziunas TF (1993) Sun, ocean, climate and atmospheric $^{14}CO_2$: an evaluation of causal and spectral relationships. Holocene 3:289–305. doi:10.1177/095968369300300401

Usoskin IG et al (2002) A physical reconstruction of cosmic ray intensity since 1610. J Geophys Res. doi:10.1029/2002JA009343

Usoskin IG et al (2005) Heliospheric modulation of cosmic rays: monthly reconstruction for 1951–2004. J Geophys Res. doi:10.1029/2005JA011250

Usoskin IG et al (2006a) Solar proton events in cosmogenic isotope data. Geophys Res Lett. doi:10.1029/2006GL026059

Usoskin IG et al (2006b) Long-term solar activity reconstructions: direct test by cosmogenic ^{44}Ti in meteorites. Astron Astrophys. doi:10.1051/0004-6361:20065803

Usoskin IG et al (2009) On the common solar signal in different cosmogenic isotope data sets. J Geophys Res. doi:10.1029/2008JA013888

van der Veen CJ et al (1999) Accumulation at South Pole: comparison of two 900-year records. J Geophys Res. doi:10.1029/99JD900501

Wagner G et al (2000) Reconstruction of the geomagnetic field between 20 and 60 kyr BP from cosmogenic radionuclides in the GRIP ice core. Nucl Instrum Methods Phys Res B. doi:10.1016/S0168-583X(00)00285-8

Wang Y-M, Lean J, Sheeley NRJ (2000) The long-term variation of the sun's open magnetic flux. Geophys Res Lett. doi:10.1029/1999GL010744

Webber WR, Higbie PR (2003) Production of cosmogenic Be nuclei in the Earth's atmosphere by cosmic rays: its dependence on solar modulation and the interstellar cosmic ray spectrum. J Geophys Res. doi:10.1029/2003JA009863

Webber WR, Higbie PR, McCracken KG (2007) Production of the cosmogenic isotopes ^{3}H, ^{7}Be, ^{10}Be, and ^{36}Cl in the earth's atmosphere by solar and galactic cosmic rays. J Geophys Res. doi:10.1029/2007JA012499